ELSEVIER

Biochimica et Biophysica Acta 1466 (2000) 221–233

BIOCHIMICA ET BIOPHYSICA ACTA
BBA

www.elsevier.com/locate/bba

Theoretical calculations of the permeability of monensin–cation complexes in model bio-membranes

Nir Ben-Tal [a], Doree Sitkoff [b], Sharron Bransburg-Zabary [a], Esther Nachliel [a], Menachem Gutman [a,*]

[a] *Department of Biochemistry, George S. Wise Faculty of Life Sciences, Tel Aviv University, Ramat Aviv 69978, Israel*
[b] *Bristol-Myers Squibb, P.O. Box 4000, Princeton, NJ 08543-4000, USA*

Received 12 October 1999; received in revised form 6 January 2000; accepted 24 January 2000

Abstract

Monensin is one of the best-characterized ionophores; it functions in the electroneutral exchange of cations between the extracellular and cytoplasmic sides of cell membranes. The X-ray crystal structures of monensin in free acid form and in complex with Na^+, K^+ and Ag^+ are known and we have recently measured the diffusion rates of monensin in free acid form (Mo–H) and in complex with Na^+ (Mo–Na) and with K^+ (Mo–K) using laser pulse techniques. The results have shown that Mo–H diffuses across the membrane one order of magnitude faster than Mo–Na and two orders of magnitude faster than Mo–K. Here, we report calculations of the translocation free energy of these complexes across the membrane along the most favorable path, i.e. the lowest free energy path. The calculations show that the most favorable orientation of monensin is with its hydrophobic furanyl and pyranyl moieties in the hydrocarbon region of the membrane and the carboxyl group and the cation at the water–membrane interface. Further, the calculations show that Mo–H is likely to be inserted deeper than Mo–Na into the bilayer, and that the free energy barrier for transfer of Mo–H across the membrane is $\sim$1 kcal/mol lower than for Mo–Na, in good agreement with our measurements. Our results show that the Mo–K complex is unlikely to diffuse across lipid bilayers in its X-ray crystal structure, in contrast to the Mo–H and Mo–Na complexes. Apparently, when diffusing across the membrane, the Mo–K complex assumes a different conformation and/or thinning defects in the bilayer lower significantly the free energy barrier for the process. The suitability of the model for treating the membrane association of small molecules is discussed in view of the successes and failures observed for the monensin system.

Keywords: Transporter; Continuum solvent model; Poisson–Boltzmann equation; Diffusion rate; Diffusion across membrane; Ionophore

1. Introduction

Monensin, a disc-like molecule of about 50 heavy atoms, is a natural antibiotic produced by *Streptomyces* sp. The antibiotic activity of monensin is attributed to its ability to exchange protons and cations in an electroneutral process. As a result, the monensin dissipates the ΔpH term of the proton mo-

Abbreviations: Mo–H, monensin in free acid form; Mo–Na, monensin in complex with Na^+; Mo–K, monensin in complex with K^+; PARSE, parameter for solvation energy; FDPB, finite difference Poisson–Boltzmann

* Corresponding author. Fax: +972-3-6415053.

0005-2736/00/$ – see front matter
PII: S0005-2736(00)00156-5

tive force without a compensating increment of the cross-membranal electric field [1]. Monensin binds cations and the X-ray crystal structures of many monensin–ion complexes have been determined [2–5]. One example, the monensin–sodium complex, is shown in Fig. 1. Monensin consists of three furan and two pyran rings. The rings are arranged in a circle with their polar oxygen atoms pointing to the cation that is buried at the center, partially screening its electric charge. The hydrophobic regions of the rings face outwards and mediate the interaction of the ion with the lipid bilayer.

Cation transport across cell membranes has been studied extensively, and the ability of monensin to accelerate the process is attributed to its ability to partition into membranes [1]. Monensin, having a negative charge, can partition into the membrane only in complex with cations. On each face of the bilayer, the monensin equilibrates with the ions according to their concentrations and their affinities for the ionophore. The unequal concentrations of the various species drive a flux of ions until the electrochemical potentials on both sides of the membrane are equal. We recently studied the kinetics of monensin-mediated cation transport across membranes using laser-induced proton pulse techniques [6]. Our main conclusion was that the diffusion rates of monensin across the membrane are not the same for all the complexes; protonated monensin (Mo–H) diffuses about 10 times faster than sodium–monensin (Mo–Na) and about 100 times faster than potassium–monensin (Mo–K). The variance in the diffusion behavior of molecules of comparable molecular weight and shape implies that their electrostatic interactions with the membrane are sufficiently different to account for the observations.

In this work, we used continuum solvent models and calculated the free energy of the monensin–cation complexes in different orientations with respect to lipid bilayers to find the minimal free energy path of each complex across the bilayer. The calculations are based on a simple model where the lipid bilayer is represented by a homogenous region of low dielectric constant embedded in the high dielectric constant of water. The monensin–cation complex is the only species that is described in atomic detail in the model. We have recently used this model for calculating the free energy of insertion of polyalanine α-helices into lipid bilayers and the results were in good agreement with experimental data [7,8]. Likewise, the present calculations are in good agreement with the kinetic measurements for the Mo–H and Mo–Na complexes. However, the calculations are fundamentally inconsistent with the available experimental data on the Mo–K complex. The discrepancy may suggest that the Mo–K complex undergoes conformational rearrangements when partitioning into bilayers.

2. Materials and methods

The total free energy difference between a molecule in the membrane and in the aqueous phase (ΔG_{tot}) can be decomposed into a sum of differences of the following energies: the electrostatic potential (ΔG_{elc}), non-polar contributions (ΔG_{np}), molecule immobilization effects (ΔG_{imm}), lipid perturbation effects (ΔG_{lip}) and the free energy of the molecule's conformational changes (ΔG_{con}) [7,9–12]:

$$\Delta G_{tot} = \Delta G_{elc} + \Delta G_{np} + \Delta G_{imm} + \Delta G_{lip} + \Delta G_{con} \quad (1)$$

We evaluate the contributions of the last three terms on the right hand side of Eq. 1 below, and in the following we focus on the first two, which we define as the solvation free energy, ΔG_{solv}

$$\Delta G_{tot} \approx \Delta G_{elc} + \Delta G_{np} \equiv \Delta G_{solv} \quad (2)$$

ΔG_{solv} is the free energy of transfer of monensin at a given conformation from water to a bulk hydrocarbon phase. It accounts for electrostatic contributions resulting from changes in the solvent dielectric constant as well as for van der Waals and solvent structure effects, which are grouped in the non-polar term and together define the classical hydrophobic effect. We calculate ΔG_{solv} using the continuum solvent model. The method has been described in detail in our earlier study of the membrane association of polyalanine α-helices [7] and in the following subsections we present a brief outline, with emphasis on the minor changes we made to adapt it to monensin.

2.1. Electrostatic contributions

The calculations are based on a continuum model in which electrostatic contributions are obtained

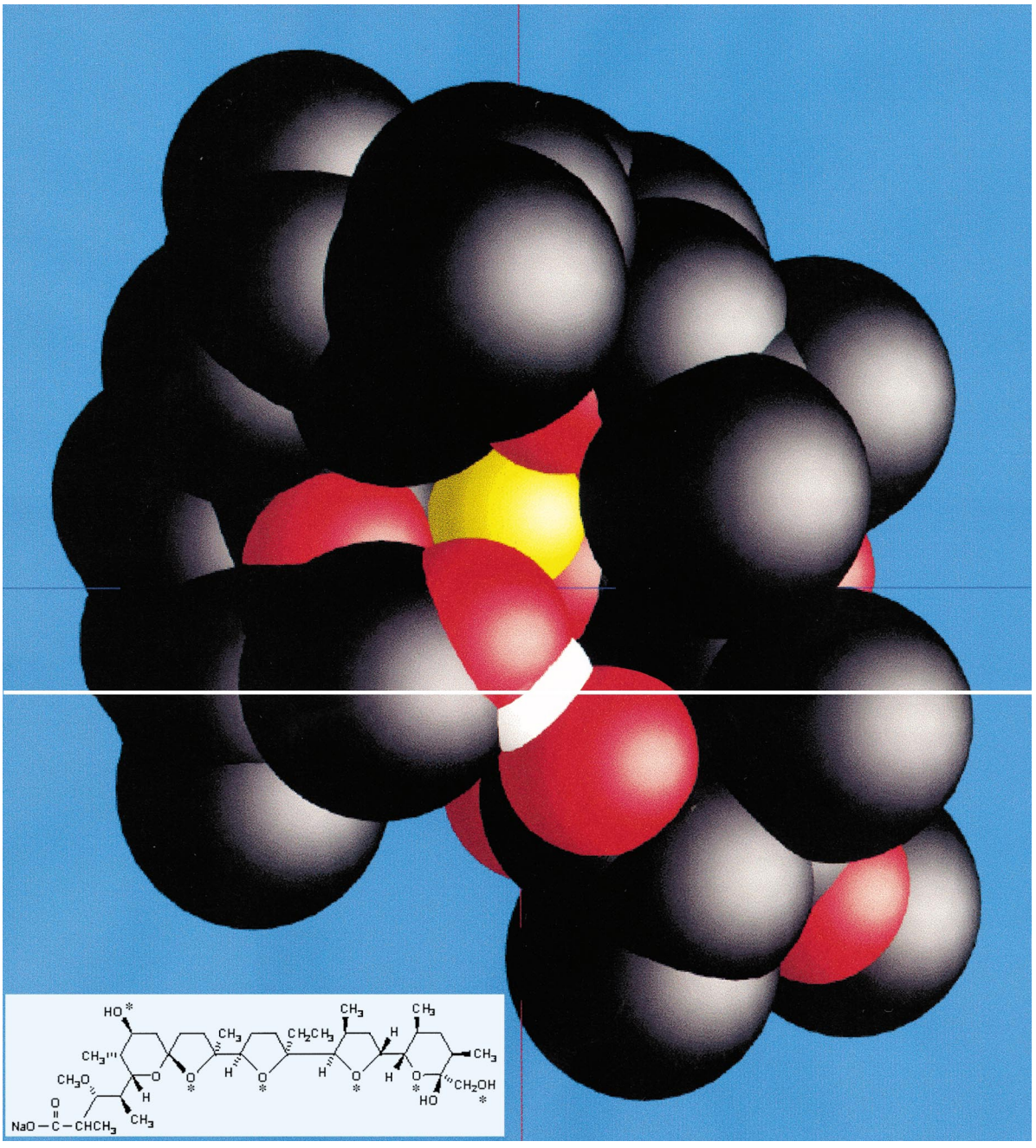

Fig. 1. Space filling model of the Mo–Na complex [4] in its most favorable orientation with respect to the lipid bilayer. Carbon atoms and methyl groups are black, oxygen atoms red, hydrogen atoms white and the Na^+ ion yellow. The white horizontal line represents the boundary between the hydrocarbon region of the lipid bilayer, above the line, and the aqueous phase below it. Notice that even though the ion is above the line, it is partially shielded from the hydrocarbon environment. The chemical structure of monensin A is presented in the frame at the bottom of the figure. The atoms marked by asterisks are in contact with the metal ion.

from finite difference solutions to the Poisson–Boltzmann equation (the FDPB method) [13,14]. We have used three monensin complexes: Mo–H, Mo–Na and Mo–K, the three-dimensional (3D) structures of which were retrieved from the Cambridge Catalogue. After retrieval, hydrogen atoms were added and the molecular structure was minimized as described below. The monensin complexes were represented in

atomic detail, with atomic radii and partial charges defined at the coordinates of each nucleus. The charges and radii were taken from a parameter set for solvation energy (PARSE), a parameter set that was derived to reproduce gas phase-to-water [15] and alkane-to-water [16] solvation free energies of small organic molecules. We recently used it to study amide hydrogen bond formation [17], polyalanine α-helices insertion into lipid bilayers [7] and helix–helix interactions in lipid bilayers [18].

The parameters for the ether group are missing in PARSE, therefore we derived partial charges to reproduce its experimentally measured solvation free energy. In the absence of direct measurement of alkane-to-water partitioning of simple ether-containing compounds, we relied on vacuum-to-water data. Vacuum-to-water solvation free energies are reported for four ether-containing molecules: dimethylether, diethylether, 2-methoxypropane and 1,2-dimethoxyethane [19]. Comparisons of solvation data of small organic molecules have revealed that alkane-to-water electrostatic solvation free energies are smaller than the corresponding gas phase-to-water free energies of transfer by a factor of 0.9 [16], and our parameterization scheme is based on this rule. Using the Pauli radii that are standard in PARSE, and by assigning partial charges of −0.73 to the ether oxygen and +0.365 to each of the two ether carbons, we reproduced the estimated experimental transfer free energies of the above compounds with less than 10% error. Standard charges of +1 and radii of 1.13 Å for sodium and 1.53 Å for potassium were assigned based on the coordination state of the ions [20].

In the FDPB calculations reported here, the boundary between the monensin complexes and the solvents (water or membrane) was set at the contact surface between the van der Waals surface of the complex and a solvent probe (defined here as having a 1.4 Å radius). The complexes and the lipid bilayer were assigned a dielectric constant of 2, whereas water had a dielectric constant of 80. The system was mapped onto a lattice of 129^3 grid points, with a resolution of four points per Å, and the Poisson–Boltzmann equation was numerically solved for the electrostatic potential. The electrostatic free energy was calculated by integration over the potential times charge distribution in space.

2.2. Non-polar contributions

The non-polar contribution to the solvation free energy, G_{np}, was assumed to be proportional to the water-accessible surface area of the monensin complex, A, through the expression

$$G_{np} = \gamma A + b \quad (3)$$

We used the parameters $\gamma = 0.0278$ kcal/(mol Å^2) and $b = -1.7$ kcal/mol that have been derived from the partitioning of alkanes between liquid alkane and water [16], and have been successfully used in our previous study [7]. The total area of the monensin complexes accessible to lipids in a particular configuration was calculated with a modified Shrake–Rupley [21] algorithm [22].

2.3. Models of monensin and the solvents

The 3D structures of the monensin–cation complexes available in the Cambridge Catalogue include only the heavy atoms, except for Mo–H [3], which is reported with all hydrogen atoms included. We added hydrogen atoms to Mo–Na [4] and Mo–K [5], and minimized the two structures using the Insight-II set of molecular modeling tools (MSI, San Diego, CA, USA). The minimization procedure, 100 steps of steepest descend, hardly affected the structures.

In the following calculations, the complexes were described in atomic detail, and were placed at different distances and orientations with respect to our model of the lipid bilayer. The bilayer was represented as a 30 Å slab with a dielectric constant of 2, known from a combination of thickness and capacitance measurements [23,24]. This is a very simplistic model of the membrane that has many limitations as discussed in [7] and below. Nevertheless, it is a standard model for the dielectric properties of the bilayer and we use it since the experimental evidence suggests that the solvation free energy is the dominant contribution to the free energy of many systems (e.g. [13,14,25–29]).

2.4. The lowest free energy path

The main objective of this work was to determine

the lowest free energy path for the transfer of the monensin–cation complexes across the bilayer. This could, in principle, be done by exhaustively searching in the configurational space. To save time, it was reasoned that the most stable orientations should be those with maximum contact area between the hydrophobic groups and the lipid, and with minimal contact area between the polar groups and the lipid. We choose the initial orientation of each monensin–cation complex accordingly, and sampled orientations generated by small rotations and translations around the initial orientation relative to the membrane normal. We then used the orientation of the most negative solvation free energy from the probing calculations (Fig. 1) throughout the study.

2.5. Estimate of ΔG_{imm}, ΔG_{lip} and ΔG_{con}

ΔG_{imm} reflects confinement of the external degrees of freedom of the monensin complex upon membrane association. Our calculations show that the two monensin–ion complexes that partition into the membrane, Mo–H and Mo–Na, are free to translate and rotate inside the lipid bilayer, suggesting that the immobilization effect should be negligibly small. In fact, one expects monensin to freely move inside the bilayer in view of its role as an ion exchanger.

ΔG_{lip} accounts for the perturbing effect of the monensin molecules on the lipid structure. It has an entropic origin and is proportional to the lipid-accessible area of monensin (e.g. [8]). The latter is small and thus the lipid perturbation effect of monensin should be rather small as well. We estimate it as zero.

The ring structure of monensin suggests rigidity but monensin has many sp^3–sp^3 bonds, about which there is considerable rotational freedom. The consistency of the conformation of monensin in the three Na^+ structures, hydrated and anhydrous forms [4] and the NaBr complex [30], indicates that the overall structure of Mo–Na is hardly influenced by crystal packing. It is, therefore, safe to assume that Mo–Na is unlikely to change its conformation upon membrane association, i.e. $\Delta G_{\mathrm{con}} \sim 0$. Unfortunately, it is difficult to estimate the stability of the Mo–H [3] and Mo–K [5] structures because each of them has been crystallized only in one from. The results shown below suggest that ΔG_{con} should be approximately zero for the Mo–H complex and very large for Mo–K. We address this issue in Section 4 below.

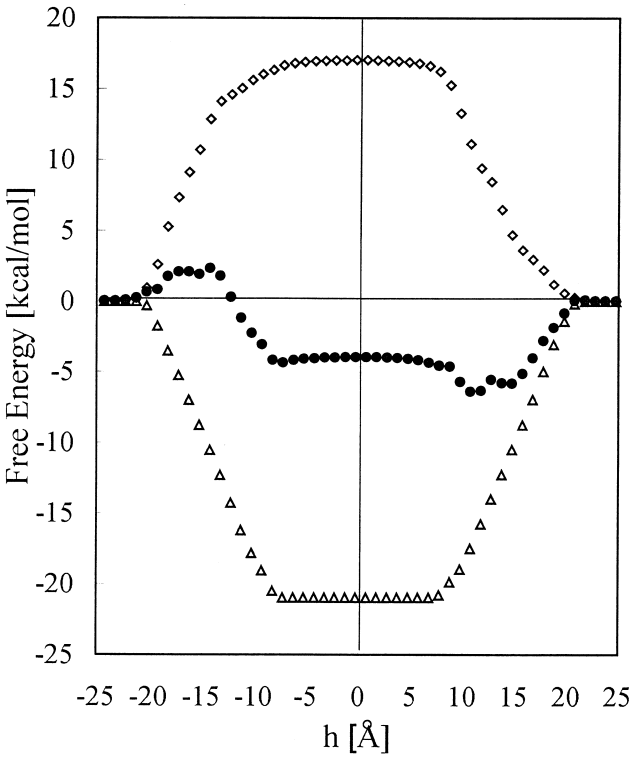

Fig. 2. Transfer of the Mo–Na complex across the bilayer. Electrostatic (◇), non-polar (△) and solvation (●) free energy curves obtained for the transfer of Mo–Na across the bilayer. h is the distance between the geometrical center of Mo–Na and the bilayer midplane along the membrane normal, and the free energy is reported relative to its value at infinite distance. See text for details.

3. Results

3.1. The insertion free energy

Fig. 2 presents the non-polar, electrostatic and solvation free energies of transfer of Mo–Na through the lipid bilayer along a hypothetical path. Mo–Na was placed at the orientation of Fig. 1, and was not allowed to rotate throughout the calculations. The zero of free energy of the Mo–Na complex was set to a configuration at which Mo–Na is infinitely distant from the membrane. The transfer starts at $h = -21$ Å, where the complex is just in contact with the bilayer. The electrostatic contributions to

the free energy become gradually more positive and the non-polar contributions more negative during the process, until they reach their maximal absolute values around $h=-7$ Å, where Mo–Na is entirely buried in the bilayer. Mo–Na is fully buried in the bilayer at -7 Å $< h < 7$ Å, and the electrostatic and non-polar contributions to the free energy are at their saturation values in this region. As the translocation process proceeds, the absolute values of the electrostatic and non-polar contributions to the free energy of transfer gradually decrease from their maximal values around $h=7$ Å to zero at $h=21$ Å, where the complex is just outside the bilayer and the process ends. The non-polar and electrostatic contributions have opposite effects on the transfer process, but their sum, the solvation free energy, is not zero because they do not fully balance each other.

Mo–Na is a fairly symmetric molecule as is evident by the symmetry of the non-polar free energy curve (triangles, Fig. 2). However, the electrostatic free energy curve of monensin is directionally biased; it is steeper for insertion in the orientation where the polar region of the complex is facing the lipid (-21 Å $< h < -7$ Å) than for reversed polarity (7 Å $> h > 21$ Å). The sum of the non-polar and electrostatic contributions is the solvation free energy, which gives a curve that is asymmetrical as well. It has a free energy minimum around $h=12$ Å, where the hydrophobic furanyl and pyranyl moieties of Mo–Na are buried in the hydrophobic core of the membrane while the carboxyl group still protrudes into the aqueous phase (Fig. 1), and a maximum at the reversed polarity of $h=-14$ Å. The latter orientation is obviously energetically unfavorable and it is most likely that Mo–Na rotates in the hydrophobic region of the bilayer and protrudes from the other side of the membrane with its carboxyl group first. Thus, the free energy curve for the transfer of the complex across the bilayer is likely to be fully symmetrical around the bilayer midplane.

3.2. The rotation of monensin–cation complexes within the membrane

The free energy minimum observed for the monensin–sodium complex in the orientation of Fig. 1 implies that the diffusion of the complex across the lipid bilayer involves a 180° rotation to reach the symmetrical stable orientation at the other end of the bilayer. The experiments of Nachliel et al. [6] support this conclusion and even provide an estimate of the rotation rate. In that study, we noted that the rate constants of the reactions between monensin and the ions are diffusion-controlled, implying that whenever a cation encounters a monensin molecule, the ionophore is already in the right configuration to bind it, i.e. the carboxylate region is facing the aqueous phase. Thus, the rotation rate of the monensin–cation complex inside the membrane is not a rate limiting step in the overall process. Based on the measured rate constants of ion binding ($k=10^{10}$ M^{-1} s^{-1}) and the ion concentration used in the experiments (0.1 M), the rotation time should be shorter than the encounter rate in Nachliel's experiment, $\tau=(0.1\ k)^{-1}=1$ ns. This rate is in accordance with the rotational diffusion of a sphere the size of monensin in a matrix of the membrane viscosity ($\eta<2$P) [31].

3.3. Comparison of the three complexes

We repeated the calculations of Fig. 2 using two other monensin–cation complexes: Mo–H and Mo–K. Our calculations show that only one of them, Mo–H, is likely to diffuse across lipid bilayers. In contrast, the crystal structure of Mo–K possesses a large electrostatic dipole that prevents the complex from immersing inside lipid bilayers ($\Delta G_{sol}\sim 40$ kcal/mol), in conflict with experimental data. This issue will be discussed further below.

The solvation free energy curves obtained for the Mo–H and Mo–Na complexes are presented in Fig. 3. It is evident from the figure that the two complexes are likely to dissolve in the bilayer, but that they are unequal in their tendency to do so; Mo–H is more likely to be inserted into the bilayer than Mo–Na. Besides the solubility difference, the free energy curves of the two complexes have similar features. Each of them shows locations of maximal and minimal stability, i.e. minima and maxima in the solvation free energy curves, respectively. The free energy minima correspond to the configurations where the hydrophobic furanyl and pyranyl moieties of the monensin are buried inside the hydrocarbon region of the bilayer while the charged or polar carboxylic group and the ion protrude into the aqueous phase

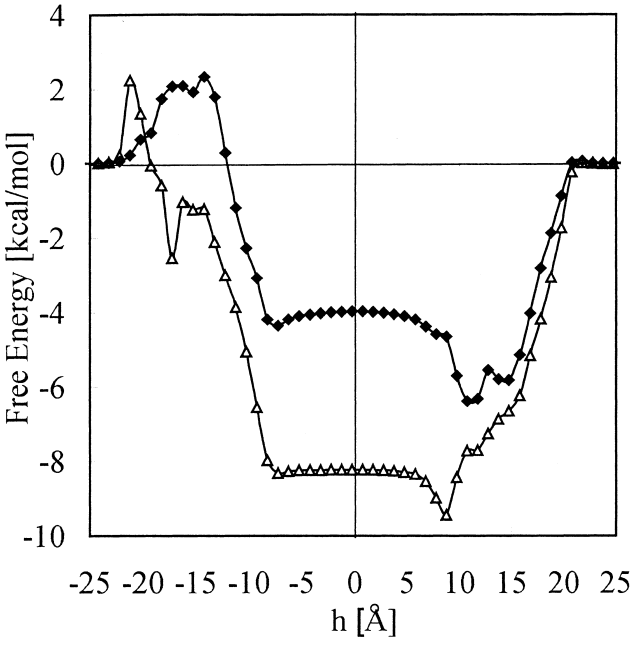

Fig. 3. Translocation of the monensin–cation complexes across the bilayer. Solvation free energy curves obtained for the transfer of Mo–H (△) and Mo–Na (◆) across the bilayer. h is the distance between the geometrical center of the complex and the bilayer midplane along the membrane normal. See text for details.

(Fig. 1). This orientation provides free energy benefits from the non-polar interactions and the least possible electrostatic free energy penalty. The reverse orientation, where the charged or polar carboxylic group is buried in the membrane and the furanyl and pyranyl groups are in the aqueous phase, is obviously unfavorable and results in the observed free energy maximum.

From our point of view, the most interesting differences between the solvation free energy curves of Fig. 3 are the relative location and local depths of the free energy minima. The free energy minima of Mo–H and Mo–Na occur at $h=9$ Å and $h=12$ Å, respectively. The depths of the corresponding local free energy minima are 1.2 and 2.3 kcal/mol. We shall relate these values to the measurements of Nachliel et al. [6] in Section 4 below.

3.4. Convergence tests

We repeated the calculations of Fig. 2 using different grid sizes (97^3, 113^3 and 129^3) and scales (2, 3 and 4 grids/Å) to test the convergence of our calculations. We also tested the effect of changing the boundary conditions from 'Coulombic' to 'Dipolar' in DelPhi. Our results show that the calculations are converged to less than 0.2 kcal/mol, which is more than sufficient for this study. Notice, however, that the high precision of our calculations is due to the simplified model we used. The neglect of the polar head groups region of the bilayer and the fixed conformation of monensin in our model may result in an error that is larger than 0.2 kcal/mol as discussed further below.

4. Discussion

Our calculations show that two of the three monensin–cation complexes, Mo–H and Mo–Na, may partition into the bilayer without deviating from their X-ray crystal structure. For these two complexes, the calculations further show that the minimal free energy paths for the translocation across the membrane are qualitatively similar (Fig. 3) and conform to the available experimental results. We focus on these two complexes in the beginning of this section and deal with the Mo–K complex below.

The calculations demonstrate that the most stable orientation of the Mo–H and Mo–Na complexes in the membrane is with the hydrophobic furanyl and pyranyl rings buried in the hydrocarbon region of the lipid bilayer and the polar carboxyl group and ion protruding into the aqueous phase (Fig. 1). Besides these common features, there are quantitative differences between the solvation free energy curves of the Mo–H and Mo–Na complexes:

1. On setting the free energy of the complex in water as a reference, the likelihood of the complexes to partition into the bilayer is not identical. Mo–H, with $\Delta G_{sol} = -9.4$ kcal/mol, is more soluble in the bilayer than Mo–Na, with $\Delta G_{sol} = -6.4$ kcal/mol. This pattern is in accord with experimental data on the stability of the complexes in organic solvents [32,33] and on the relative membrane affinities of the cation complexes [1].
2. The most likely location of the complex in the bilayer depends on the cation. The Mo–H complex is almost fully buried inside the bilayer at $h=9$ Å, where only one of the etheric oxygen

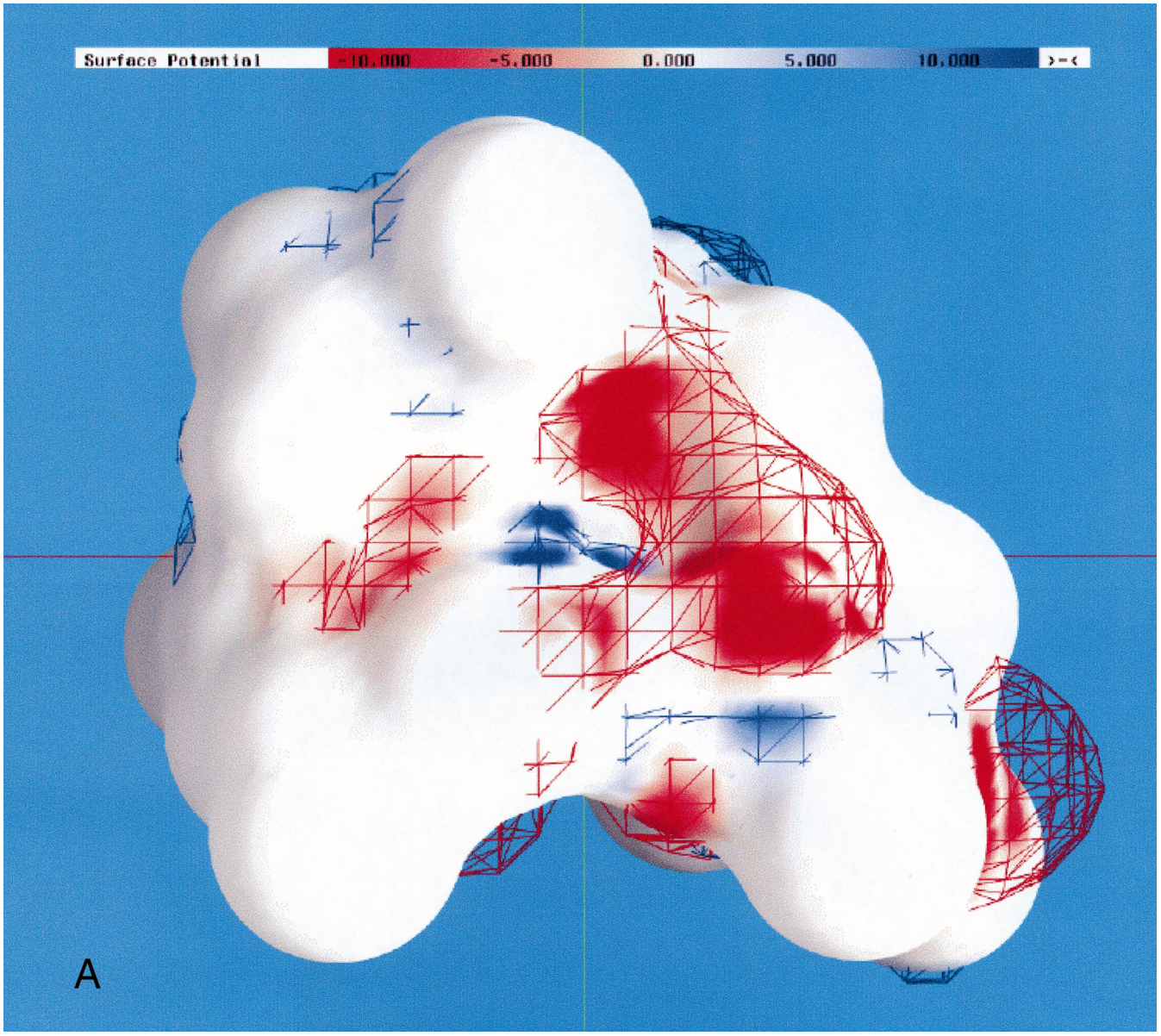

Fig. 4. Surface potential of the monensin complexes. (A) Mo–H, (B) Mo–Na and (C) Mo–K. Potentials more positive than +10 *kT*/e are deep-blue, potentials more negative than −10 *kT*/e are deep-red and neutral potentials (0 *kT*/e) are white. 3D contours of the potential at + and −1 *kT*/e are shown in blue and red mesh. The level of polarity of each complex is reflected both in the ratio of colored vs. white region of the molecular surface and by the proximity of the contours to the molecular surface; polar complexes are characterized by large patches of red and blue on their molecular surface and by the fact that their contours are far from the molecular surface. It is obvious from the figure that Mo–K is significantly more polar than Mo–H and Mo–Na. The figure was generated by the GRASP program [38].

atoms extends into the aqueous phase. On the other hand, the Mo–Na complex has a preferred position closer to the interface, where the ion is in the low dielectric phase and the carboxylate protrudes into the high dielectric water phase.

3. The height of the free energy barrier for membrane crossing varies in accordance with the experimental results; the free energy barrier observed for the Mo–H complex is lower than the barrier observed for Mo–Na. The local free energy well, out of which the Mo–H complex has to emerge in order to diffuse towards the midplane

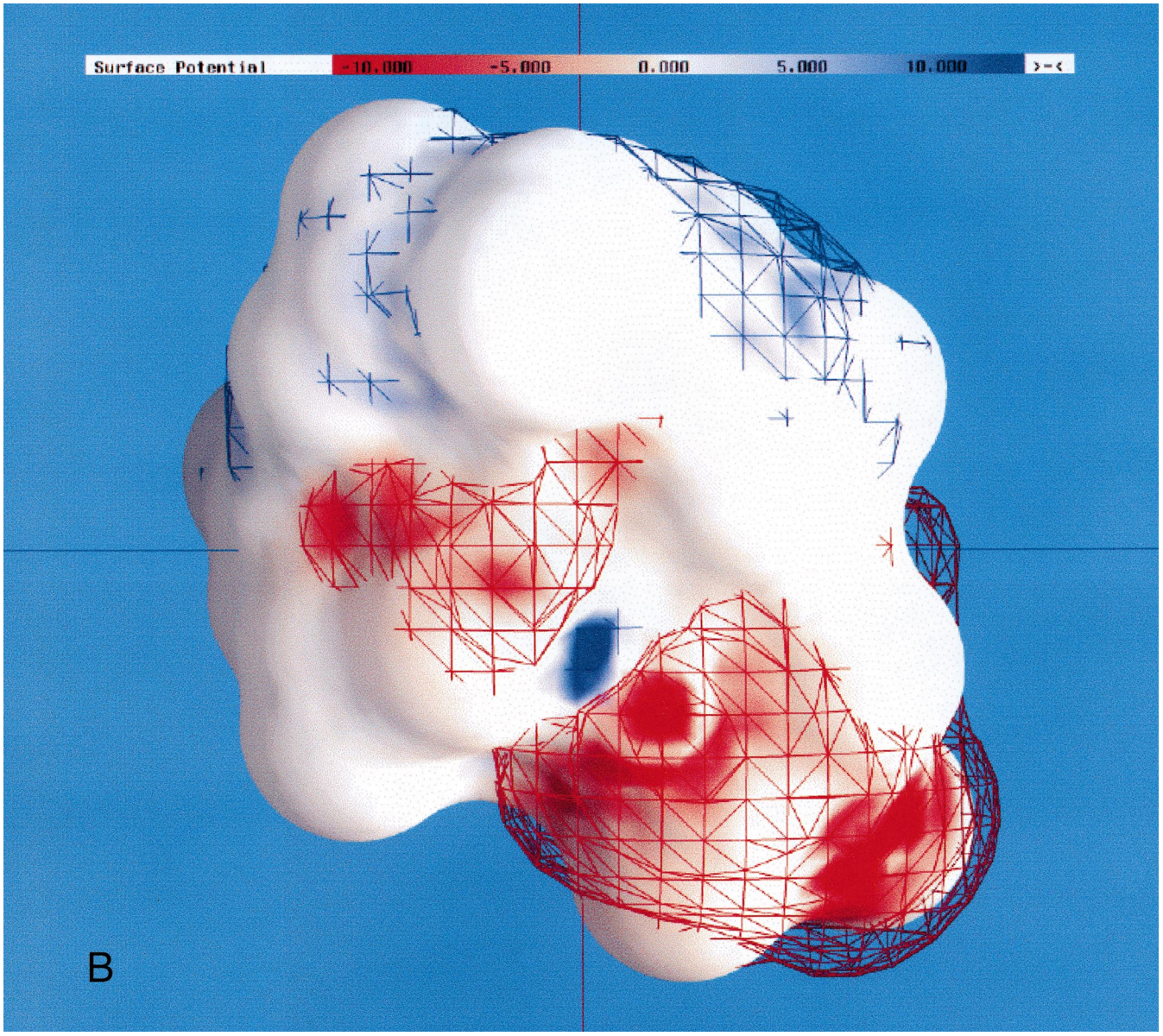

Fig. 4 (*continued*).

of the membrane, is ~1.2 kcal/mol (Fig. 3). This implies that thermal energy can easily dislodge Mo–H from its favored location near one face of the membrane sending it over to diffuse across the membrane where (after rotation) it will occupy a symmetric orientation near the other face of the membrane. The calculated free energy barrier for Mo–Na is ~2.3 kcal/mol, i.e. 1.1 kcal/mol higher than that of the Mo–H complex, in nearly perfect agreement with the value of 0.96 kcal/mol that has been calculated from the kinetic analysis of Nachliel et al. [6].

The variations in membrane–water partitioning and in the location and depth of the local minima in the membrane are mostly due to the electrostatic potential of the complexes. Fig. 4A–C depicts the electrostatic surface potential of the three complexes, and the differences between them reflect the site of cation binding. The two metal ions, K^+ and Na^+, are

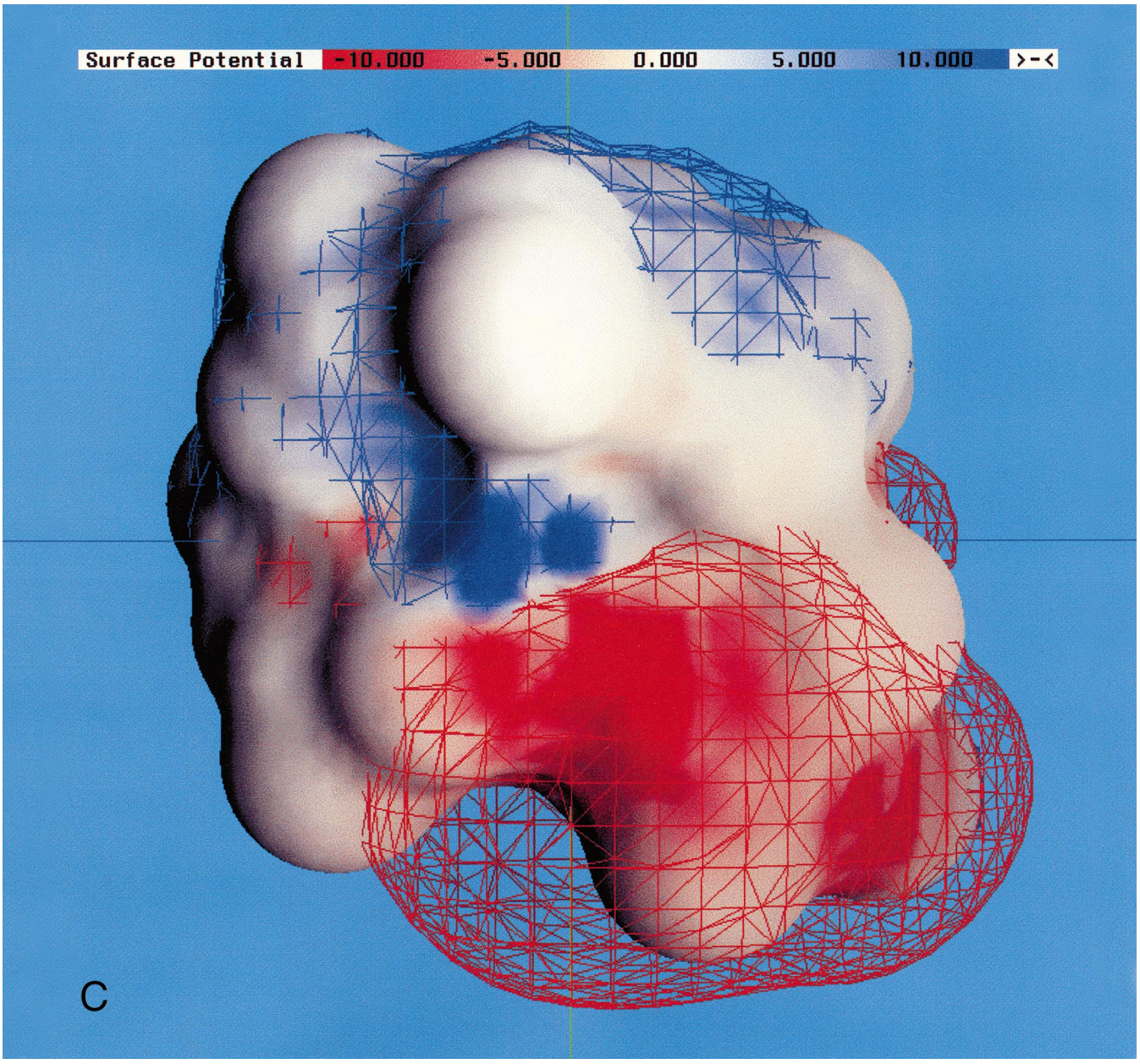

Fig. 4 (*continued*).

encapsulated by the furanyl and pyranyl rings of monensin and the carboxylate group is not in metal-binding coordination. In contrast, the X-ray crystal structure of Mo–H shows that the proton is covalently linked to the carboxylate, effectively neutralizing its charge, and involved in a hydrogen bond in the hydrogen bonds network of Mo–H. For these reasons, the polarity of the protonated monensin is the smallest of all three, it has relatively small patches of positive and negative electrostatic potentials, and its +1 kT/e and −1 kT/e iso-potential contours occur near its molecular surface (Fig. 4A). The Mo–Na complex (Fig. 4B) is slightly more polar than the Mo–H molecule, as evident by the larger patches of positive and negative potential and from the fact that its iso-potential contours occur far from the molecular surface. The Mo–K complex (Fig. 4C) is significantly more polar than the other two complexes due to its larger ionic radius that distorts the structure of monensin [5].

The present set of calculations is complementary to our previous experimental study, in which we measured the rate constants of the elementary processes of the monensin-mediated ion exchange mechanism. Evidently, the outcome of the free energy profiles yields results that corroborate the experimentally derived estimates of the rate constants, and suggests a molecular interpretation of the elementary processes involved in monensin-mediated cation transport across biological membranes. However, the model has a number of limitations that we outline in the following paragraphs.

The main limitation of our model is that the conformation of the monensin–ion complex is taken as a given, and thus we are practically bound to use only the crystal structures that were experimentally determined by X-ray crystallography. Such conformations are, presumably, the most stable under the specific conditions selected for growing the crystals (e.g. the type of solvent and the solute density), but may not necessarily be the most stable in all phases. For example, our calculations show that the membrane translocation of the Mo–K complex in its X-ray crystal structure involves a solvation free energy penalty of about 40 kcal/mol. Since the available experimental data indicate that Mo–K does diffuse across bilayers [6], we conclude that the membrane-associated conformation of the complex is different than that of the X-ray structure and/or thinning defects significantly reduce the free energy barrier for the process [34].

A related shortcoming of our model is the assumption that the conformation of the monensin–ion complex remains unchanged throughout the transfer from the aqueous phase to the bilayer. Monensin is a small molecule and its membrane-associated conformation may be slightly different from its form in aqueous solutions. The smallness of monensin suggests that the energetic costs of such a conformational change may be small compared to its effect on the solvation free energy. The consistency of the monensin conformation in the three Mo–Na crystals indicates that the overall structure of Mo–Na is very little influenced by crystal packing. Thus, we feel safe to assume that Mo–Na is unlikely to change its conformation upon membrane association. We cannot state with the same confidence that Mo–H does not go through conformational changes in the transition from the aqueous phase into the lipid bilayer because only one crystal form of Mo–H has been observed. Moreover, there is no direct evidence that its conformation in any of these phases is similar to the X-ray structure. However, the agreement between the calculations and the kinetic measurements is an indirect support that Mo–H does not change its conformation upon binding or that the conformational changes have little effect on the free energy curve of Fig. 3.

The description of the lipid bilayer as a slab of low dielectric constant obscures all atomic detail about monensin–bilayer interactions. However, this minimalistic model of the dielectric properties of the hydrocarbon region of the membrane successfully accounts for the effects of the aqueous phase on charged and polar groups that are buried in the membrane [7,35–36].

While the slab model is an acceptable approximation for calculating the water–membrane partitioning of uncharged molecules, it might be inadequate for calculating the water-to-membrane transfer free energy of ion-containing complexes, such as Mo–Na and Mo–K. To explore this possibility, we repeated the calculations of Fig. 2 for the Mo–Na complex with a different charge distribution between the central cation and the surrounding oxygen atoms. By comparing the results of these calculations with the original free energy curve described above, we get an upper bound estimate of the contribution of the Na^+ ion to solvation. To this end, we eliminated the +1 charge of the Na^+ ion and in parallel changed the partial charge of each of the four coordinated oxygen atoms from -0.73 to -0.48 for compensation. The free energy curve thus obtained was very similar to the original curve; the minimum occurred at the same configuration, i.e. $h = 12$ Å, and its depth changed by ~ 1.5 kcal/mol only. We conclude that, due to the coordination of the oxygen atoms around the cation, the monensin complex has practically no ionic nature (Fig. 4B).

The greatest uncertainty in the slab model results from its complete neglect of the polar head groups region, which is presumably the most favorable site of the monensin–cation complexes. Since the dielectric constant in this region is estimated to be between 25 and 40 [37], the polar head groups region might

most appropriately be regarded as part of the aqueous phase defined in this study.

The most crucial factor in the present calculations is the charge distribution on the monensin–cation complexes, which is determined by the assignment of the atomic partial charges from the PARSE parameter set. However, because PARSE yields accurate transfer free energies between water and liquid alkane for small organic molecules including ethers and carboxylic acids (both charged and neutral), it seems reasonable to assume that it provides a good approximation to the water–membrane solvation properties of monensin complexes that are constructed from the same chemical groups.

Monensin is a small drug molecule that exerts its effect by wrapping a hydrophobic surface around charged ions to facilitate their diffusion across the cell membrane. A large number of hydrophobic compounds, such as drugs, hormones and vitamins, used to modulate biological activities have to propagate through membranes, to bind to their targets. In this respect, monensin can be viewed as a representative of a large group of entities and our model may enable us to screen their conformations with respect to the membrane association and permeation, e.g. the crystal structures of Mo–H and Mo–Na vs. that of Mo–K. Our experience from the studies on the monensin–cation complexes is that relatively small conformational changes, involving minor changes in the internal energy, lead to large changes in the solvation free energy. Thus, combining the model with tools for sampling conformations, such as molecular dynamics simulations or ab initio quantum mechanical calculations, may provide a valuable method for screening small molecule libraries to suggest candidates that are likely to partition into lipid bilayers and to estimate their rate of diffusion across the bilayer. The main strength of our model is that, while it takes into account the atomic details of the small drug molecule, it does not require a detailed description of the membrane. The neglect of detailed description of the lipid bilayer typically leads to less accurate calculations, but it also makes the model general and readily applicable for screening the membranal permeability of small molecules of potential therapeutic capabilities.

Acknowledgements

The work started while M.G. was a visiting Professor in the laboratory of Prof. Barry Honig. We wish to thank Prof. Honig for his generous hospitality and for helpful discussions. This research was supported by Grant number 683/97-1 from the Israel Science Foundation and by fellowships from the Wolfson and Alon Foundations to N.B.-T.

References

[1] B.C. Pressman, Ionophorous antibiotics as models for biological transport, Fed. Proc. 27 (1968) 1283–1288.
[2] M. Pinkerton, L.K. Steinrauf, Molecular structure of monovalent metal cation complexes of monensin, J. Mol. Biol. 49 (1970) 533–546.
[3] W.K. Lutz, F.K. Winkler, J.D. Dunitz, Crystal structure of the antibiotic monensin. Similarities and differences between free acid and metal complex, Helv. Chim. Acta 54 (1971) 1103–1108.
[4] W.L. Duax, G.D. Smith, P.D. Strong, Complexation of metal ions by monensin Crystal and molecular structure of hydrated and anhydrous crystals forms of Monensin–Na, J. Am. Chem. Soc. 102 (1980) 6725–6729.
[5] W. Pangborn, W.L. Duax, D. Langs, The hydrated Potassium complex of the ionophore Monensin A, J. Am. Chem. Soc. 109 (1987) 2163–2165.
[6] E. Nachliel, Y. Finkelstein, M. Gutman, The mechanism of monensin-mediated cation exchange based of real time measurements, Biochim. Biophys. Acta 285 (1996) 131–145.
[7] N. Ben-Tal, A. Ben-Shaul, A. Nicholls, B. Honig, Free-energy determinants of α-helix insertion into lipid bilayers, Biophys. J. 70 (1996) 1803–1812.
[8] A. Ben-Shaul, N. Ben-Tal, B. Honig, Statistical thermodynamic analysis of peptides and protein insertion into lipid membranes, Biophys. J. 71 (1996) 130–138.
[9] D.M. Engelman, T.A. Steitz, The spontaneous insertion of proteins into and across membranes: the helical hairpin hypothesis, Cell 23 (1981) 411–422.
[10] F. Jahnig, Thermodynamics and kinetics of protein incorporation into membranes, Proc. Natl. Acad. Sci. USA 80 (1983) 3691–3695.
[11] R.E. Jacobs, S.H. White, The nature of the hydrophobic binding of small peptides at the bilayer interface: implications for the insertion of trans-bilayer helices, Biochemistry 28 (1989) 3421–3437.
[12] M. Milik, J. Skolnick, Insertion of peptide chains into lipid membranes: an off-lattice Monte Carlo dynamics model, Proteins 15 (1993) 10–25.
[13] B. Honig, K. Sharp, A.-S. Yang, Macroscopic models of aqueous solutions: biological and chemical applications, J. Phys. Chem. 97 (1993) 1101–1109.

[14] B. Honig, A. Nicholls, Classical electrostatics in biology and chemistry, Science 268 (1995) 1144–1149.
[15] D. Sitkoff, K.A. Sharp, B. Honig, Accurate calculation of hydration free energies using macroscopic solvent models, J. Phys. Chem. 98 (1994) 1978–1988.
[16] D. Sitkoff, N. Ben-Tal, B. Honig, Calculation of alkane to water solvation free energies using continuum solvent models, J. Phys. Chem. 100 (1996) 2744–2752.
[17] N. Ben-Tal, D. Sitkoff, I.A. Topol, A.-S. Yang, S.K. Burt, B. Honig, The free energy of amide hydrogen bond formation in vacuum, in water and in liquid alkane solutions, J. Phys. Chem. B 101 (1997) 450–457.
[18] N. Ben-Tal, B. Honig, Helix-helix interactions in lipid bilayers, Biophys. J. 71 (1996) 3046–3050.
[19] C. Hansch and A. Leo, Substituent Constants for Correlation Analysis in Chemistry and Biology, Wiley, New York, 1979.
[20] J.E. Huheey, E.A. Keiter and R.L. Keiter, Inorganic Chemistry, Harper Collins, New York, 1993, p. 72.
[21] A. Shrake, J.A. Rupley, Environment and exposure to solvent of protein atoms. Lysozyme and insulin, J. Mol. Biol. 79 (1973) 351–371.
[22] S. Sridharan, A. Nicholls, B. Honig, A new vertex algorithm to calculate solvent accessible surface area, Biophys. J. 61 (1992) A174.
[23] R. Fettiplace, D.M. Andrews, D.A. Hatdon, The thickness composition and structure of some lipid bilayers and nutural membranes, J. Membr. Biol. 5 (1971) 277–296.
[24] J.P. Dilger, R. Benz, Optical and electrical properties of thin monoolein lipid bilayers, J. Membr. Biol. 85 (1985) 181–189.
[25] J. Kyte, R.F. Doolittle, A simple method for displaying the hydropathic character of a protein, J. Mol. Biol. 157 (1982) 105–132.
[26] D. Eisenberg, A.D. McLachlan, Solvation energy in protein folding and binding, Nature 319 (1986) 199–203.
[27] A. Warshel, Computer Modeling of Chemical Reactions in Enzymes and Solutions, John-Wiley and Sons, New York, 1991.
[28] K. Yue, A.K. Dill, Folding proteins with a simple energy function and extensive conformational searching, Protein Sci. 5 (1996) 254–261.
[29] J.A. McCammon, Theory of biomolecular recognition, Curr. Opin. Struct. Biol. 8 (1998) 245–249.
[30] D.L. Ward, K.-T. Wei, J.C. Hoogerheide, A.I. Popov, The crystal and molecular structure of the sodium bromide complex of monensin, $C_{36}H_{62}O_{11}.Na^{+}Br^{-}$, Acta Cryst. B34 (1987) 110–115.
[31] M.K. Jain and R.C. Wagner, Introduction to Biological Membranes, Wiley and Sons, New York, 1980.
[32] B.G. Cox, N.G. vanTruong, J. Rzeszotarska, H. Schneider, Rates and equilibria of alkali metals and silver ion complex formation with monensin in ethanol, J. Am. Chem. Soc. 106 (1984) 5965–5969.
[33] P.J.F. Henderson, J.D. McGivan, J.B. Chappel, The action of certain antibiotics on Mitochondrial, Erythrocyte and artificial phospholipids membranes, J. Biochem. 111 (1969) 521–535.
[34] M.A. Wilson, A. Pohorille, Mechanism of unassisted ion transport across membrane bilayers, J. Am. Chem. Soc. 118 (1996) 6580–6587.
[35] S. Berneche, M. Nina, B. Roux, Molecular dynamics simulation of melittin in a dimyristoylphosphatidylcholine bilayer membrane, Biophys. J. 75 (1998) 1603–1618.
[36] P. LaRocca, Y. Shai, M.S. Sansom, Peptide-bilayer interactions: simulations of dermaseptin B, an antimicrobial peptide, Biophys. Chem. 76 (1999) 145–159.
[37] R.G. Ashcroft, H.G. Coster, J.R. Smith, The molecular organisation of bimolecular lipid membranes. The dielectric structure of the hydrophilic/hydrophobic interface, Biochim. Biophys. Acta 643 (1981) 191–204.
[38] A. Nicholls, K.A. Sharp, B. Honig, Protein folding and association: insights from the interfacial and thermodynamic properties of hydrocarbons, Proteins 11 (1991) 281–296.